scientific reports

Check for updates

OPEN

Proteomic analysis reveals selenium-induced metabolic alterations in forest-grown ginseng

Junwei Wang[1]✉, Mei Lv[2]✉ & Siyao Wang[3]✉

Selenium (Se) enriched forest-grown ginseng is famous for its high Se content and excellent protein quality, which are necessary for varieties of metabolic processes and play an important role in both ginseng growth and its health benefits for humans. However, the regulatory mechanism underlying Se enrichment and molecular responses of forest-grown ginseng after application of exogenous Se is still unclear. This study investigated the effect of Se fertilizer on molecular changes in physiological metabolisms of forest-grown ginseng during the growth process by analyzing differentially expressed proteins (DEPs). The results showed that 371 proteins were significantly changed under application of Se fertilizer. Further KEGG pathway analysis indicated that the DEPs are primarily involved in carbon metabolism, biosynthesis of amino acids, protein processing in endoplasmic reticulum, phenylpropanoid biosynthesis, oxidative phosphorylation and spliceosome. The expression levels of ATP sulfurylase, adenosine 5′-phosphosulfate reductase, nitrate reductase, nitrite reductase, superoxide dismutase, catalase, and H^+-ATPase were up-regulated in ginseng treated with Se, and these key DEPs were mainly related to the maintenance of cellular membrane, antioxidant capacity and resistance to stresses. These findings reveal the nutritional and functional differences and establish a theoretical basis for further research on protein biological functions in forest-grown ginseng.

Keywords Selenium, Proteomic analysis, Ginseng, Metabolic changes

Forest-grown ginseng (*panax ginseng* Meyer), a well-known medicinal plant known for its pharmacological efficacy, is widely grown in the northeast of China[1–3]. It has been used in the medical system of East Asian countries due to its homeostatic effects and various pharmacological properties, including improvements in brain function, anti-tumor activity, anti-aging, and blood pressure control[4–6]. In recent years, the quality of ginseng products, including saponins, amino acid, alkaloids and trace mineral elements, has attracted increasing attention. Among these product quality indexes, the content of Se has been greatly favored because it positively affects many functions[7–9], promotes ginseng growth, and play a positive role in the health of edible people.

As a metalloid element, Se has unique properties in many aspects. This element is considered an essential micronutrient, present in organisms as the amino acid selenocysteine (SeCys), which is incorporated into the catalytic sites of indispensable selenoproteins[10]. These selenoproteins are mainly involved in detoxification and scavenging of reactive oxygen species (ROS)[11]. It has been reported that Se-rich ginseng cultivated in Se-rich nutrient solution has a high effective utilization rate of Se and may exhibit high anticancer activity[12]. Moreover, a selenylation-modified polysaccharide was yielded by nitric acid-selenious acid modified method from ginseng extract markedly inhibiting the growth of human promyelocytic leukemia HL-60 cells via induction of apoptosis[13]. It is of great significance for the study of it in human and plant systems. Nowadays, the promoting effects of Se on plant physiology and the mechanism of plant absorption of Se have attracted increasing attention.

Se uptake from the environment depends on a number of factors, such as the concentration, form, and activity of Se in the soil, as well as the plant's physiological metabolism. For example, plant root cells can absorb selenate, selenite and organic selenium compounds such as SeCys and SeMet, but not selenates or colloidal elemental Se[14]. Moreover, Se can have either good or bad effects on plants depending on its concentration[10]. Trace amounts of Se can promote the growth and physiological metabolism of plants, while high concentration of Se has adverse effects on plants[15,16]. The absorption of Se by plants mainly depends on many key metabolic

[1]College of Grain Science and Technology, Shenyang Normal University, Shenyang 110034, People's Republic of China. [2]Institute of Agro-Products Processing Science and Technology, Shenyang Academy of Agricultural Sciences, Shenyang 110025, People's Republic of China. [3]School of Public Health, Shenyang Medical College, Shenyang 110034, People's Republic of China. ✉email: synuwjw@163.com; lnsylm2011@126.com; wangsiyao2021@symc.edu.cn

pathways, such as its primary and secondary metabolisms[14], nutrient transport metabolism[17], antioxidant metabolism[18], energy metabolism[19], etc., which involve many physiological components. Previous studies have focused on the importance of Se by evaluating physiological and biochemical characteristics. However, the absorption, physiology and regulatory mechanism of Se in forest-grown ginseng remain unclear.

In this study, the protein changes accompanying Se absorption during the growth of forest-grown ginseng were analyzed using TMT protein labeling and LC-MS/MS. These results facilitate the identification of dynamic patterns in the differential expression of proteins, along with the construction of protein functional networks, during the uptake of Se from the external environment, which not only offers valuable reference for efficient cultivation and protein-based development, but also lays a solid theoretical foundation for further optimizing cultivation conditions and enhancing the medicinal value of forest-grown ginseng.

Materials and methods

Plant materials and Se treatment

The cultivation and Se fertilizer treatment of forest-grown ginseng were carried out in a ginseng experimental planting base in Benxi, Liaoning province, China (41.03°N, 123.52°E). A total of 1,200 ginseng in 1998 m^2, were divided into two groups each containing 3 replicates. After five years of growing, treated group was applied with Se fertilizer every 7 d between April and July, while control group was applied with distilled water. The concentration of Se was 4 mg/kg, which was selected as the best option from previous experiment (data were not shown). The experimental growth period of ginseng was 3 years. After growth, cultivated 8-year-old forest-grown ginseng samples were collected and frozen in liquid nitrogen for further biochemical and molecular index analysis. Take 10 ginseng from each parallel sample in each group. The measurement of Se content and protein extraction using a mixed sample of 10 pieces of ginseng.

Measurement of Se content

Ginseng samples (1.0 g) were placed into a digestion tube, adding 10 ml mixture of HNO_3 and $HClO_4$ (9:1), and was covered with a surface dish for cold digestion overnight. The next day, the sample was heated on an electric heating plate, and promptly supplemented with HNO_3 until the solution became clear. After cooling, the digestion liquid was added with 5 ml HCl (6 mol L^{-1}), and continue to heat until the solution became clear and colorless with white smoke. After cooling again, the samples were mixed with 2.5 ml 100 g L^{-1} potassium ferricyanide, and then diluted to 10 ml with deionized water. The Se concentration was determined by hydride atomic fluorescence spectrometry (HG-AFS). The results are expressed as mg kg^{-1} fresh weight (FW).

Protein extraction

Samples of ginseng were chopped and ground in liquid nitrogen, and then lysed in a lysis buffer containing 0.1 mol L^{-1} NH_4HCO_3 (pH 8.0), 0.2% SDS and 6 mol L^{-1} Urea. After 5 min of ultrasonic treatment, the sample was centrifuged at 12,000 g at 4 °C for 15 min, and then the supernatant was transferred to a clean test tube. The extracts of the samples were reduced using 0.002 mol L^{-1} DTT at 56 °C for 1 h, and alkylated in darkness with sufficient iodoacetamide for 1 h at room temperature. The samples were mixed with 4 times the volume of pre-cooled acetone by vortexing, incubated at -20 °C for 2 h, and then the precipitation was collected by centrifugation. After being washed twice with cold acetone, the pellets were dissolved in a solution containing 0.1 mol L^{-1} bicarbonate triethylammonium (TEAB, pH 8.5) and 6 mol L^{-1} urea. Protein concentrations were determined by using the Bradford protein assay.

Peptide preparation and TMT labeling

Each sample supernatant, which contained exactly 0.1 mg of protein, was digested with Trypsin Gold (Promega) at a 1:50 enzyme-substrate ratio. After digestion at 37 °C for 16 h, the high urea was removed by the desalination of C18 cartridge. Then the desalted peptides were dried by vacuum centrifugation and were labeled with TMT6/10-plex reagents (TMT6/10plex™ Isobaric Label Reagent Set, Thermo Fisher). Labeling reagent (1 unit), dissolved in 41 µL of acetonitrile, was used for 0.1 mg of peptide, which was dissolved in 100 µL of 0.1 mol L^{-1} TEAB. The incubation time was 1 h, and ammonium hydroxide was used to stop the reaction. The peptides with different labels were mixed and then desalted with a spin column (Thermo Fisher, 89852).

HPLC-MS/MS analysis

Fractionation of the TMT-labeled peptide mixture was operated by using an HPLC (L3000, Rigol) equipped with a C18 column (Waters BEH C18 4.6 × 250 mm, 5 µm). The conditions of HPLC were as follows: mobile phase A was 2% acetonitrile and phase B was 98% acetonitrile; flow rate of mobile phase was 1 ml/min; column oven was 50 °C. A gradient elution was performed as followed: 3% B, 0 min; 3–5% B, 10 min; 5–20% B, 20 min; 20–40% B, 18 min; 40–50% B, 2 min; 50–70% B, 3 min; 70–100% B, 1 min; 100-0%, 4 min, 0% B, 12 min. The eluent was monitored at UV 214 nm, one tube per minute, and incorporated into 10 fractions. The obtained fractions were then dried in vacuum and recombined in 0.1% (v/v) formic acid for then subsequent analysis.

An EASY-nLCTM 1200 UHPLC system (Thermo Fisher) equipped an Orbitrap Q Exactive HF-X mass spectrometer (Thermo Fisher) performed in data-dependent acquisition (DDA) mode was used for the shotgun proteomics analysis. The conditions were as follows: the ion mode was positive polarity mode; the spray voltage was set as 2.3 kV, with capillary temperature at 320 °C; the full MS scanning range was from 350 m/z to 1500 m/z; the resolution was 60,000 (200 m/z); the target value of automatic gain control (AGC) was 3 × 106; the maximum ion injection time was 20 ms.

A total of 40 precursor ions with the abundant from full MS scan were selected for secondary mass spectrometry by using higher energy collisional dissociation (HCD). The resolution was set as 15,000 (200 m/z),

and the target value of AGC was 1 × 105, with a normalized collision energy of 32%, a maximum ion injection time of 45 ms, an intensity threshold of 8.3 × 103, and dynamic exclusion parameter of 20 s.

Proteome data processing

The result spectra of each fragment were separately searched in ginseng genome database (http://ginsengdb.snu.ac.kr/data.php) by search engine: Proteome Discoverer 2.2 (PD 2.2, Thermo). The significant ratio was defined as $p < 0.05$, and fold change ≥ 1.2 or ≤ 0.83 were used to screen the DEPs. Analysis of Gene Ontology (GO) and InterPro (IPR) of DEPs were performed with the interproscan-5 program against the non-redundant protein database. The family and pathway of proteins were analyzed by using the databases Clusters of Orthologous Groups (COG) and Kyoto Encyclopedia of Genes and Genomes (KEGG). The STRING-db server based (http://string.embl.de/) on related species was used to predict possible interaction partners. The enrichment analysis of GO, IPR and KEGG was carried out by using the enrichment pipeline[20].

RNA isolation and cDNA synthesis

Total RNA was extracted from frozen ginseng sample (1 g) by using an RNAprep Pure Plant (Polysaccharide & Polyphenolics-rich) kit (Tiangen, Beijing, China). Total RNA concentration was determined according to the absorbance at 260 nm, and the integrity of RNA was confirmed by 1.0% agar-gel electrophoresis. The first strand of cDNA for real-time q-PCR analysis was synthesized by using a TIANScript RT kit (Tiangen).

Real-time q-PCR assays

Q-PCR analysis was performed to validate the gene expression of DEPs by using an iQ5 real-time PCR system (Bio-Rad, USA). The operation parameters were set up according to the instructions of RealMasterMix (SYBR Green) (Tiangen) as follows, 30 s at 95°C, 40 cycles of 5 s at 95°C, and 34 s at 58°C. β-actin gene (5'-CGTGATCT TACAGATAGCTTGATGA-3' and 5'-AGAGAAGCTAAGATTGATCCTCC-3') was used as an internal control to normalize small differences in template amounts. Primers were designed by Primer Premier 5.0 software according to relevant genes, as shown in Table 1. Three replicates were performed for each sample.

Statistical analyses

A completely random design was performed with three biological replicates. Analysis of variance (ANOVA) was performed using SPSS software. At the 5% level, significant differences were determined by Duncan's multi-range test.

Results

Content of Se

The content of Se in forest-grown ginseng under the treatment of exogenous Se fertilizer for 3 years was compared with that of the control group. To avoid the influence of maturity and other factors on differential proteomics results, samples with no significant difference in size or weight were selected from the control and treated groups for further analysis. The results of Se content in ginseng are shown in Fig. 1. From the results, we found that Se concentration was 0.19 mg kg^{-1} in Se-treated ginseng, which was significantly higher than that in the control ginseng (0.059 mg kg^{-1}). As a result, ginseng demonstrated powerful abilities to accumulate Se during the 3-year Se fertilizer application.

Identification and annotation analysis

In this study, 37,378 unique peptides and 7,278 proteins were identified, among which 7,271 proteins were quantified from ginseng samples. Venn diagram of comparative Gene Ontology (GO), Clusters of Orthologous Groups of Proteins (COG), Kyoto Encyclopedia of Genes and Genomes (KEGG), and Inter pro (IPR) domain annotations are presented in Fig. 2A. To better understand their functions, 5,259 proteins were annotated with GO terms (Fig. 2B). In particular, oxidation-reduction involved 538 proteins under the biological process. In

Protein	Accession number	Forward primer (5′-3′)	Reverse primer (5′-3′)	Product size (bp)
APS (ATP sulfurylase)	Pg_S0682.30	AAATTGGCTCATTGGTGGAG	TGACCATTGTGCACAGGATT	165
APR (adenosine 5'-phosphosulfate reductase)	Pg_S0277.37	TCCTCAGCTGGGATCATTTC	AACCTCTTCAGGAGCAACGA	163
SiR (sulfite reductase)	Pg_S5909.2	GCATGGGTTCAACTCTTGGT	CTCTCTCCATCCACCCACAT	172
CyS (cysteine synthase)	Pg_S0015.6	AACATTGCAAAGGGTTCTGC	CTAGGCCAATGCCTGTGTTT	181
CGS (cystathionine γ-synthase)	Pg_S7062.1	ATCACATTGCAATCCGTCAA	ATTATTGCTGGCTGGTCCAC	163
CBL (cystathionine β-lyase)	Pg_S0741.54	CCGGGTGAAGGAGGTTTATT	GGGACTTCACACTCCCAAAA	185
MTR (methionine synthase)	Pg_S3712.7	ACATGGAGAGCCAGAGAGGA	CGACGACCAGAAGACAGTCA	172
GCL (glutamate-cysteine ligase)	Pg_S1116.11	ACTGTCCTTCCGGGACTTTT	GGCAATGCACATAACCTCCT	174
GSH (glutathione synthase)	Pg_S0017.2	GTGGGCTTGTTGTTGGAGAT	GTTCTGGAAAGCGAGTCCTG	205
NR (nitrate reductase)	Pg_S2647.5	CTGCCACGTTACAGTGTGCT	TCAACATGTTTCCCACCTGA	190
NiR (nitrite reductase)	Pg_S4339.13	GCCCGAGCCACATATTCTAA	ATATCGGCCACTTGAACCTG	198
H^+-ATPase (ATP synthase)	Pg_S3025.3	CCTCCTGATGCTATGGGAAA	AACTCGCTGCCCTGTAAGAA	195

Table 1. Primers for Real-time q-PCR Analysis.

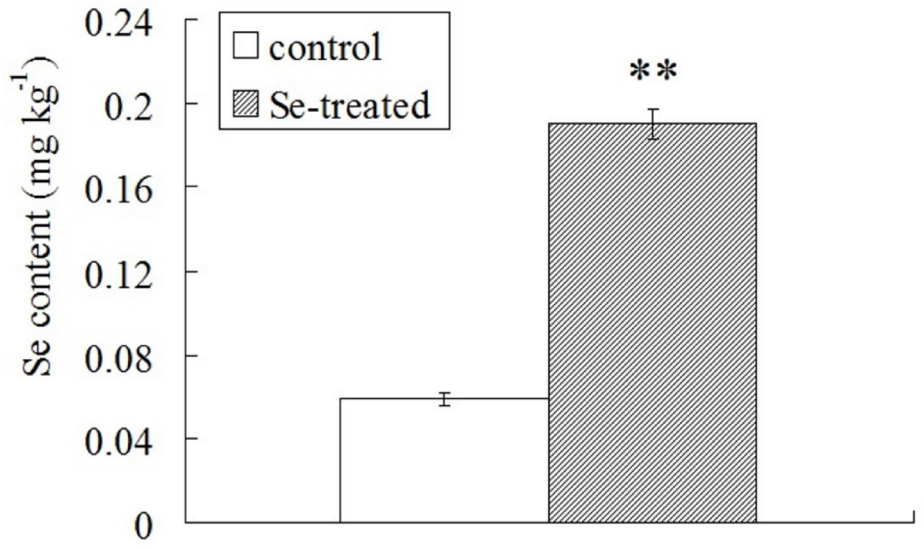


Fig. 1. Content of Se in ginseng. Means ± SE of three replicates are shown.

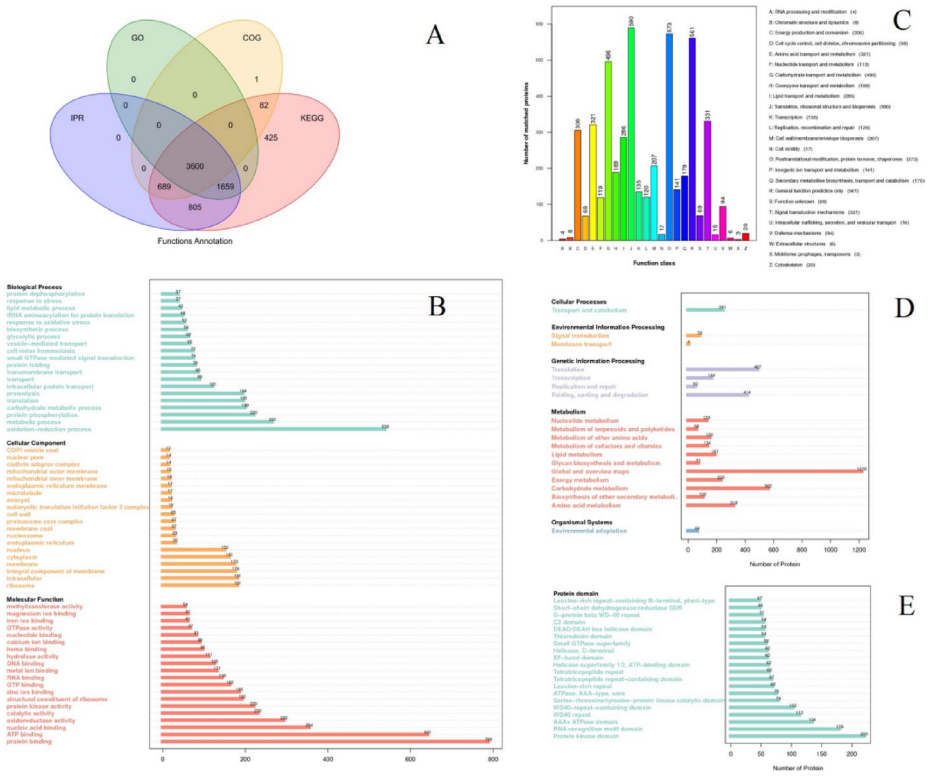


Fig. 2. Functional annotation of identified proteins. (**A**) Venn diagram of function annotation. (**B**) GO annotation. (**C**) COG annotation. (**D**) KEGG annotation. (**E**) IPR annotation.

cellular component, 181 proteins were annotated under intracellular and ribosome, respectively. In the molecular function category, 788 proteins were annotated under protein binding.

Moreover, 4,372 proteins underwent annotation through COG functional classification. The major functional classifications included translation, ribosomal structure and biogenesis, represented by 590 proteins; posttranslational modification, protein turnover, and chaperones, with 573 proteins; general function prediction only, accounting for 561 proteins; and carbohydrate transport and metabolism, featuring 496 proteins (Fig. 2C). Simultaneously, 7,260 proteins were annotated across diverse KEGG pathways. Among these, metabolic pathways contained the largest number of annotated proteins, reaching 3,159 (Fig. 2D). In addition, 6,752 proteins were

annotated with various IPR expressions. Among them, the protein kinase domain had the highest number of IPR-annotated proteins, with 220 proteins (Fig. 2E).

Enrichment analysis

In comparing control samples with Se-treated samples, proteins exhibiting FC ≥ 1.2 or ≤ 0.83 and $p < 0.05$ were considered as differentially accumulated. Overall, 371 proteins were identified. Among these proteins, 239 were down-regulated and 132 were up-regulated in Se-treated samples compared with control samples (Fig. 3A). Moreover, the DEPs in the two groups were analyzed and shown in the form of hierarchical clustering heat map (Fig. 3B). Color blocks in distinct positions on the heat map denoted the relative expression levels of proteins at the corresponding positions. Specifically, red signified high expression, while blue indicated low expression. Evidently, the heat map demonstrated a clear pattern of separation in DEP profiles between the two sample groups.

The above 371 DEPs showed significant differences in molecular function during different biological processes ($p < 0.05$). They were mainly divided into 46 functional categories of GO, of which 19 are biological processes, 9 are cellular components and 18 are molecular functions (Fig. 3C). GO enrichment analysis revealed that the DEPs were mainly involved in 'response to stress', 'cell wall organization or biogenesis' and 'response to oxidative stress' in the annotation of biological processes (Fig. 4A). In terms of cellular component annotation, the most of the DEPs participated in 'protein complex', 'intracellular organelle part' and 'nucleus' (Fig. 4B). Analysis of molecular function annotation showed that the DEPs were mostly involved in 'DNA binding', 'heme binding' and 'iron ion binding' (Fig. 4C).

The enrichment pathway of DEPs was investigated by KEGG enrichment analysis. The results of KEGG enrichment analysis showed that DEPs were mainly mapped to 56 pathways, of which 20 metabolic pathways with the largest amount of enriched proteins were shown in Fig. 3D. In ginseng, the metabolic pathway with the highest number of enriched DEPs was the metabolic pathways category, with 62 DEPs. This was followed by the biosynthesis of secondary metabolites pathway, which had 35 DEPs, and the carbon metabolism pathway, which contained 19 DEPs. Ten proteins were involved in the phenylpropanoid biosynthesis, with the lowest p value among the identified pathways.

Protein-protein interaction network analysis

A physical and functional protein-protein interaction (PPI) network was established by using STRING v.11.0 online software. In the PPI network, DEPs formed a total of 231 known or predicted interactions (Fig. 5). The results of the protein interaction network prediction showed that glyceraldehyde 3-phosphate dehydrogenase (Pg_S3350.2), S-adenosylmethionine synthetase (Pg_S1400.29), DNA topoisomerase (Pg_S6276.3), and enolase (Pg_S3731.15) had a key role in the network. The highest number of interactions was detected for heat shock protein (Pg_S0649.4).

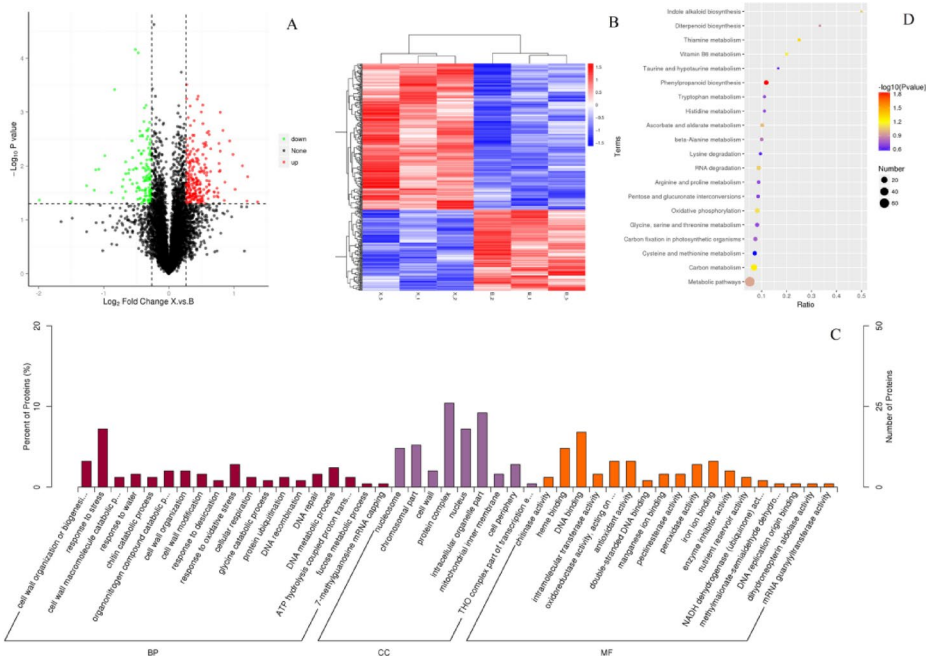


Fig. 3. Analysis results of DEPs. (**A**) The volcano plot shows the up- (red) or down-regulated (green) proteins. (**B**) Hierarchical clustering of DEPs. Scale bar in blue and red represents the decrease and increase of the identified protein level, respectively. (**C**) GO enrichment analysis. (**D**) KEGG enrichment analysis. X represents samples of Se-treated group, and B represents samples of control group.

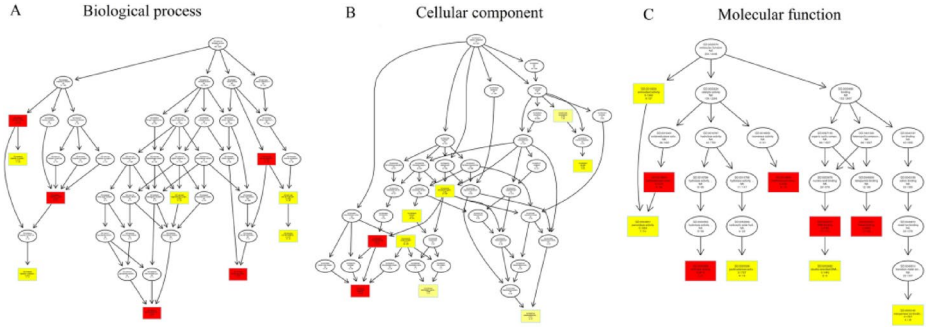


Fig. 4. Directed acyclic graph (DAG) of GO enrichment analysis. Top10 of the result of GO enrichment analysis was selected as the main node of DAG, and the associated GO terms are displayed together through the inclusion relation. (**A**) Biological process. (**B**) Cellular component. (**C**) Molecular function. The depth of color represents the degree of enrichment. X represents samples of Se-treated group, and B represents samples of control group.

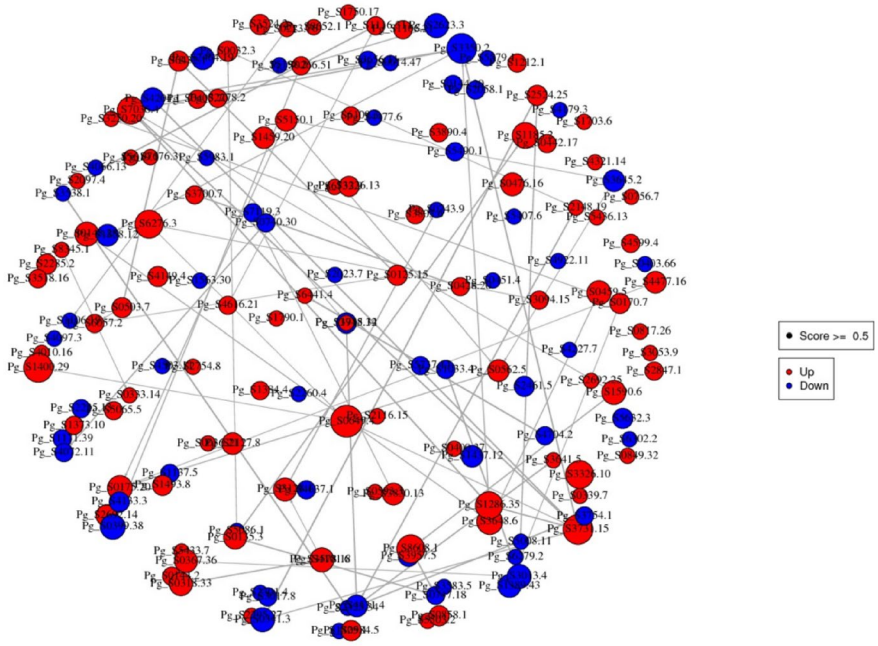


Fig. 5. Network of predicted protein-protein interactions. X represents samples of Se-treated group, and B represents samples of control group.

Validation of proteins identified by real-time PCR analysis

To validate the results of TMT, we carried out real-time PCR to analyze transcript levels of DEPs. Figure 6 shows the differential up-regulation fold changes in both transcript levels and TMT-based protein levels for the 12 proteins, comparing the Se-enriched treatment group to the control group. The 12 proteins h include important proteins that function in selenocompound metabolism, energy metabolism, cysteine and methionine metabolism, glutathione metabolism, nitrogen metabolism, oxidative phosphorylation, and transport and catabolism pathways. The expression levels of the selected protein transcripts were consistent with the TMT data, indicating that the genes exhibited both similar protein and mRNA expression patterns. For example, the mRNA level of the gene of APS increased by 2.11-fold, which was similar to the 2.3-fold increase in protein expression. The mRNA level of GCL increased by 2.07-fold, which was higher than the 1.8-fold increase in the protein expression level as detected by the TMT analysis. Real-time PCR results showed that the protein and mRNA expression patterns of these genes were similar, but the expression levels were slightly different.

Discussion

Se is an essential mineral element for humans and animals, and the main intake route of Se comes from plants[21]. Exogenous application of Se can not only increase the concentration of Se in edible parts of plants, but also promote the growth of plants[21–23]. This study conducted a comparative proteomic analysis at 8 years of ginseng

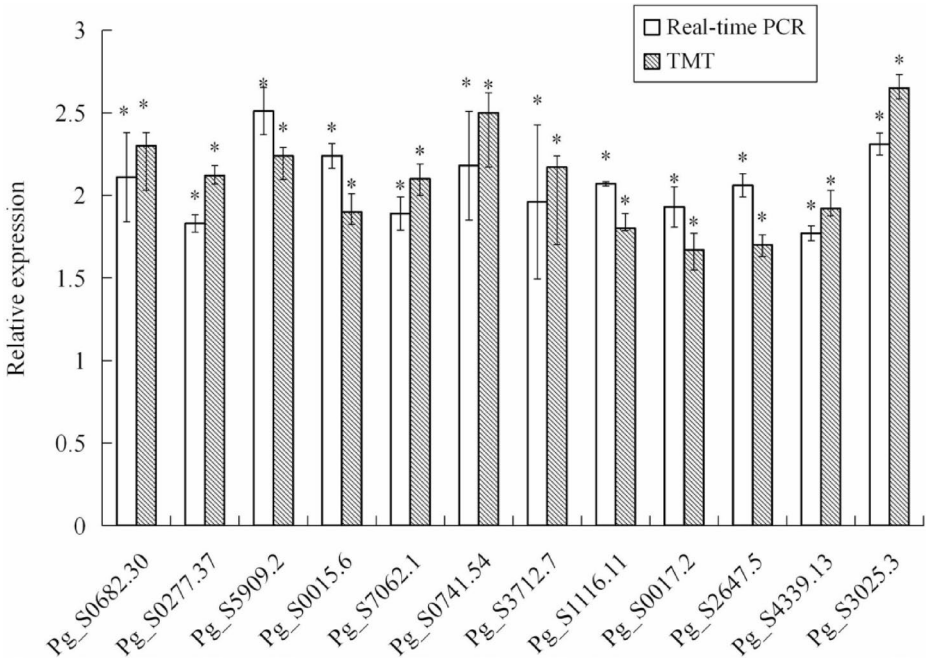


Fig. 6. Comparative analysis of RNA and protein levels of DEPs detected by real-time PCR and TMT. Means ± SE of three replicate experiments are shown. * denote statistically significant differences ($p < 0.05$).

that had been treated with Se for 3 years and naturally grown ginseng to preliminarily explore the molecular basis of Se treatment's effects on ginseng growth. Based on a comparison at a single time point, captures a proteomic network of the stabilized adaptive state reached after Se treatment. The results showed that exogenous Se fertilizer application played a dramatic role in promoting ginseng growth. In addition, Se content in ginseng treated with 3 years of Se fertilizer was 3.2 times that in the control group. Se content of ginseng in Se fertilizer treated group complies with national standards for selenium-enriched foods in Chi, and poses no risk of selenium-induced adverse effects when consumed within the normal range[24–25]. The results of our study suggested a Se uptake and assimilation system in ginseng. However, the mechanisms of absorption and translocation of this mineral element are complex and regulated by many molecular factors. Meanwhile, the stimulatory effect of Se intake on the physiological and metabolic processes of ginseng is also realized by regulating a series of metabolic pathways, which involve the differential expression of many proteins.

This study preliminarily revealed key metabolic pathways potentially involved in ginseng's response to Se treatment. The first important metabolic pathway involved in the uptake of Se from the external environment is the primary and secondary metabolism of Se in plants, which contains several key enzymes. ATP sulfurylase (APS), which is a key enzyme involved in the first step of the sulfate pathway, can also regulate the first step of Se metabolism[19]. Some selenate that enters the cytosol can be converted to adenosine 5'-phosphoenolate by the presence of APS in the cytosol[14]. In plasmid, selenate is converted into adenosine 5'-phosphoenolate and then selenite through the activities of APS and adenosine 5'-phosphosulfate reductase (APR)[14,26]. In our study, two APS (Pg_S3650.10 and Pg_S0682.30) were significantly induced (1.92-fold and 2.3-fold, respectively), and two APR (Pg_S0277.37 and Pg_S0661.5) were also found to be up-regulated by 2.12-fold and 1.88-fold, respectively. Meanwhile, differentially expressed sulfite reductase (SiR) (Pg_S5909.2), which can reduce selenate to selenite, as well as a cysteine synthase (CyS) (Pg_S0015.6), which catalyzes the formation of selenocysteine (SeCys) from selenide and O-acetylserine, were also detected to be 2.24-fold and 1.9-fold up-regulated. In the metabolic pathway of Se in plants, elenomethionine (SeMet) is formed from SeCys under the continuous catalysis of cystathionine γ-synthase (CGS), cystathionine β-lyase (CBL) and methionine synthase (MTR)[27]. In the present study, two CGS (Pg_S0061.28, Pg_S7062.1) were found to be 1.98-fold and 2.1-fold up-regulated, respectively. In addition, a CBL (Pg_S0741.54) and a MTR (Pg_S3712.7) were also significantly up-regulated (2.5-fold and 2.17-fold, respectively). Moreover, major secondary metabolites of Se, such as selenoglutathione, and selenosugars, can be derived from SeCys and SeMet under the catalysis of numerous key enzymes[28–29]. In this study, a glutamate-cysteine ligase (GCL) (Pg_S1116.11) and a glutathione synthase (GSH) (Pg_S0017.2), which catalyze the synthesis of selenoglutathione from SeCys, were significantly induced by 1.8-fold and 1.67-fold, respectively. These up-regulated proteins in the primary and secondary metabolic pathways may be important factors associated with Se enrichment in ginseng. In ginseng treated with exogenous selenium fertilizer, the metabolic pathways of glycine, serine, and threonine metabolism was down-regulated, which indicates that selenium treatment may have inhibited the photorespiration of ginseng and reprogrammed the carbon and nitrogen flows, shifting resources more from basal growth to the antioxidant and stress defense systems. In carbohydrate transport and metabolism, including β-galactosidase (Pg_S1798.6) and pectate lyase (Pg_S4133.3)

were down-regulated by Se treatment, which indicates that selenium treatment may have improved the stability of the cell wall and enhance the ginseng's resistance.

N, P, and K are important growth substances for organisms, which can determine the level of plant nutrients and growth status of plants. Previous studies revealed that Se application affected N, P, and K accumulation in some plants, and some key enzymes play an important role in this process[30–31]. The present proteomic data showed the differential expression trend of some of these proteins under Se treatment. Plants obtain nitrogen mainly through nitrate and ammonium ions. The nitrate ions absorbed by plants are degraded into ammonium ions by the catalytic action of nitrate reductase (NR) and nitrite reductase (NiR), the key enzymes of nitrate metabolism, and are combined with organic molecular structure[32–33]. On the other hand, Ammonium ions can be directly integrated into organic form as glutamine and glutamate under the catalysis of glutamine synthetase (GS) and glutamate synthase (GOGAT), and then serve as the nitrogen donors provided for the biosynthesis of all the essential amino acids[32]. In this study, a NR (Pg_S2647.5) and a NiR (Pg_S4339.13) were up-regulated by 1.7-fold and 1.92-fold, respectively. Meanwhile, two GS (Pg_S5638.3; Pg_S1703.32) and three GOGAT (Pg_S0442.17; Pg_S0536.6; Pg_S2580.1) were detected to be significantly induced. In addition, two nitrate transporter proteins (Pg_S1003.16; Pg_S1306.26) and an ammonium transporter protein (Pg_S0590.5), which may play a crucial role in the process of nitrate and ammonium transportation, were also up-regulated by 1.76-fold, 1.8-fold and 1.85-fold under Se treatment. Phosphate transporter (PHT) can improve the efficiency of plant phosphorus nutrient[34], which is a structural component of nucleic acids and participates in enzyme regulation as well as in energy metabolism[35], and plays important roles in physiological modification of photosynthesis rate in plants[36]. In this study, three PHT (Pg_S8709.2, Pg_S1202.14 and Pg_S0930.25) involved in the phosphorus-related metabolic pathways were up-regulated in Se-treated ginseng. In terms of potassium-related metabolic pathways, a potassium channel protein (KCP, Pg_S1124.24) and a potassium transporter protein (KTP, Pg_S1750.18) were also significantly increased under Se treatment. These results suggest that exogenous Se fertilizer treatment may promote the growth process of ginseng by modulating nutrient absorption, transport, and utilization. Excess accumulation of the reactive oxygen species (ROS) under the stress of adversity may cause oxidative damage to some key molecules[37], and promote the deterioration of the membrane compartmentalisation system in plants[38]. It was reported that the salt stress-mediated oxidative damage in wheat seedling was reduced under Se supplementation by up-regulating the activity of enzymatic components of the antioxidant system such as superoxide dismutase (SOD), catalase (CAT), ascorbate peroxidase (APX), glutathione reductase (GR) and glutathione S-transferase (GST)[37]. Similarly, Se supplementation reduced H_2O_2 content and strengthened the antioxidant enzymes in rice[39], oilseed rape[40] and groundnut[41]. In the present study, a total of an SOD (Pg_S2608.12), two CAT (Pg_S0213.11, Pg_S3613.4), an APX (Pg_S1832.3), a GR (Pg_S0093.7), two GST (Pg_S2473.2, Pg_S0756.7, Pg_S2097.4), and four POD (peroxidase Pg_S3641.5, Pg_S2148.19, Pg_S1116.31, Pg_S1715.32) involved in antioxidant pathways were significantly up-regulated in Se-treated ginseng, which can indicate the enhancement of anti-oxidation ability of cells and the maintenance of cellular membrane compartment distribution, to improve the resistance to varieties stress in the growth process of ginseng.

Energy levels of cells energy levels play an important role in maintaining the normal physiological metabolism of organisms. Adequate cellular energy has a close relation with some important physiological and biochemical processes, such as nutrients absorption[42–43], antioxidant activity, and photosynthesis[44] in plants. Exogenous calcium alleviated the inhibition induced by acid rain on the activity of plasma membranes H^+-ATPase (ATP synthase), which benefited in maintaining uptake of nutrients[45]. It also reported that increased antioxidative activity in mung bean sprouts might be resulted by the increasing activity of ATPases, as well as higher adenosine triphosphate (ATP) and energy charge (EC)[46]. In our study, two H^+-ATPase (Pg_S3025.3, Pg_S6026.1) which are involved in energy metabolism pathways were found up-regulated by 2.65-fold and 2.36-fold. Our results showed that Se-treated ginseng kept a higher level of H^+-ATPase compared to that of control, implying a potential function in better maintaining the electrochemical potential gradient, which may be associated with the enhanced nutrient uptake, antioxidant capacity, and energy metabolism-driven processes linked to Se treatment.

Conclusion

Our proteomic study offers a preliminary, systemic overview of the protein expression changes in ginseng during Se enrichment. A total of 371 proteins related to Se absorption and metabolism were identified between the two samples, belonging to protein complex, intracellular organelle part and nucleus. These DEPs were mainly involved in BP and MF, demonstrating that exogenous Se treatment had a great association with on protein biosynthesis and functions during the growth of ginseng. Furthermore, KEGG enrichment analysis further indicated that the number of DEPs involved in metabolic pathways, biosynthesis of secondary metabolites, and carbon metabolism was the largest. The expression levels of ATP sulfurylase, adenosine 5'-phosphosulfate reductase, nitrate reductase, nitrite reductase, superoxide dismutase, catalase, and H^+-ATPase were up-regulated in Se-treated ginseng. Consequently, it is speculated that the maintenance of cellular membrane compartment distribution and the high antioxidant capacity of cells, along with the resistance to various stresses, were enhanced. These changes, in turn, could potentially induce coordinated improvements in both primary and secondary metabolism related to Se, as well as in nutrient absorption, transport, and utilization in ginseng. The information obtained in this study is of certain reference value for future prediction of the function of these proteins and provides a reliable theoretical basis for exploring feasible regulation technologies to develop Se-enriched products. Future research will therefore focus on the functional verification, precise composition, structure, biological activity, and mechanistic regulation of these key protein candidates. Such efforts will contribute to uncovering its medicinal mechanisms and application potential.

Data availability

All data generated in this research on the proteomics of ginseng Se-enrichment process, such as protein expression profiles, differentially expressed protein lists, and statistical analysis results, are provided within the main text.

Received: 24 April 2025; Accepted: 6 March 2026
Published online: 17 March 2026

References

1. Zhang, M. et al. Multiomics joint analysis reveals the potential mechanism of differences in the taproot thickening between cultivated ginseng and mountain-cultivated ginseng. *BMC Genom.* **25**, 1228. https://doi.org/10.1186/s12864-024-11146-9 (2024).
2. Zhang, W. et al. Mechanism of sodium nitroprusside regulating ginseng quality. *Sci. Rep.* **15**, 1562. https://doi.org/10.1038/s41598-025-85905-3 (2025).
3. Wu, D. et al. Temperature seasonality and soil phosphorus availability shape ginseng quality via regulating ginsenoside contents. *BMC Plant. Biol.* **24**, 824. https://doi.org/10.1186/s12870-024-05518-2 (2024).
4. Khademian, M. & Bunch, R. The geography of wild American ginseng in North Carolina, USA: a comparative study of four capability analysis methods. *GeoJournal* **89**, 190. https://doi.org/10.1007/s10708-024-11123-5 (2024).
5. Alipanah-Moghadam, R. et al. Protective effect of Panax ginseng extract on cisplatin-induced AKI via downregulating cell death associated genes. *Sci. Rep.* **15**, 3233. https://doi.org/10.1038/s41598-025-87447-0 (2025).
6. Li, J. et al. Herbal materials used as soil amendments alleviate root rot of *Panax ginseng*. *Sci. Rep.* **14**, 23825. https://doi.org/10.1038/s41598-024-74304-9 (2024).
7. Hegab, R. H., Eissa, D. & Abou-Shady, A. Effects of foliar application of selenium and potassium-humate on oat growth in Baloza, North Sinai, Egypt. *Sci. Rep.* **12**, 15119. https://doi.org/10.1038/s41598-022-19229-x (2022).
8. LeBlanc, K. L. et al. Determination of selenium-containing species, including nanoparticles, in selenium-enriched *Lingzhi* mushrooms. *Anal. Bioanal Chem.* **416**, 2761–2772. https://doi.org/10.1007/s00216-023-05031-9 (2024).
9. Shi, T. et al. Generation of selenium-rich wheat mutants and exploration of responsive genes for selenium accumulation. *Plant. Cell. Rep.* **43**, 132. https://doi.org/10.1007/s00299-024-03219-6 (2024).
10. Schiavon, M. et al. Selenium accumulation and metabolism in algae. *Aquat. Toxicol.* **189**, 1–8. https://doi.org/10.1016/j.aquatox.2017.05.011 (2017).
11. Bulteau, A. L. & Chavatte, L. Update on selenoprotein biosynthesis. *Antioxid. Redox Sign.* **23**, 775–794. https://doi.org/10.1089/ars.2015.6391 (2015).
12. Chen, H. et al. The Anticancer Activity and Mechanisms of Ginsenosides. *Updated Rev. eFood.* **1**, 226–241. https://doi.org/10.2991/efood.k.200512.001 (2020).
13. Liao, K. N. et al. A selenium-modified ginseng polysaccharide promotes the apoptosis in human Promyelocytic leukemia (HL-60) cells via a mitochondrial-mediated pathway. *Biol. Trace Elem. Res.* **177**, 64–71. https://doi.org/10.1007/s12011-016-0879-9 (2017).
14. White, P. J. Selenium metabolism in plants. *BBA-Gen Subj.* **1862**, 2333–2342. https://doi.org/10.1016/j.bbagen.2018.05.006 (2018).
15. Li, N. N. et al. Comparative effects on nutritional quality and selenium metabolism in two ecotypes of *Brassica rapa* exposed to selenite stress. *Environ. Exp. Bot.* **150**, 222–231. https://doi.org/10.1016/j.envexpbot.2018.03.023 (2018).
16. Kolbert, Z. et al. Plant selenium toxicity: Proteome in the crosshairs. *J. Plant. Physiol.* **232**, 291–300. https://doi.org/10.1016/j.jplph.2018.11.003 (2018).
17. Bhadwal, S. & Sharma, S. Selenium alleviates physiological traits, nutrient uptake and nitrogen metabolism in rice under arsenate stress. *Environ. Sci. Pollut Res.* **29**, 70862–70881. https://doi.org/10.1007/s11356-022-20762-5 (2022).
18. Lu, Y. M. et al. Effect of foliar application of selenite on organic Se and antioxidant activity in kiwifruit. *Appl. Fruit Sci.* **66**, 1777–1785. https://doi.org/10.1007/s10341-024-01167-9 (2024).
19. Li, C. Y. et al. Methyl jasmonate maintained antioxidative ability of ginger rhizomes by regulating antioxidant enzymes and energy metabolism. *Sci. Hortic.* **256**, 108578. https://doi.org/10.1016/j.scienta.2019.108578 (2019).
20. Huang, D. W., Sherman, B. T. & Lempicki, R. A. Bioinformatics enrichment tools: paths toward the comprehensive functional analysis of large gene lists. *Nucleic Acids Res.* **37**, 1–13. https://doi.org/10.1093/nar/gkn923 (2009).
21. Titov, A. F. et al. Role of Selenium in Plants, Animals, and Humans. *Biol. Bull. Rev.* **12**, 189–200. https://doi.org/10.1134/S2079086422020104 (2022).
22. Abouelhamd, N. et al. Impact of foliar spray with Se, nano-Se and sodium sulfate on growth, yield and metabolic activities of red kidney bean. *Sci. Rep.* **13**, 17102. https://doi.org/10.1038/s41598-023-43677-8 (2023).
23. Wang, H. et al. Effects of Foliar Application of Nano-Se on Photosynthetic Characteristics and Se Accumulation in *Paeonia ostii*. *Russ J. Plant. Physiol.* **71**, 117. https://doi.org/10.1134/S1021443724605111 (2024).
24. Polyzos, S. A. et al. Selenium and selenoprotein P in nonalcoholic fatty liver disease.Horm. *-Int J. Endocrinol. Metab.* **19**, 61–72. https://doi.org/10.1016/j.redox.2020.101519 (2020).
25. Liu, C. et al. Potential Applications and Risks of Supranutritional Selenium Supplementation in Metabolic Dysfunction-Associated Steatotic Liver Disease: A Critical Review. *Nutrients* **17** (15), 2484. https://doi.org/10.3390/nu17152484 (2025).
26. Lima, L. W., Pilon-Smits, E. A. H. & Schiavon, M. Mechanisms of selenium hyperaccumulation in plants: A survey of molecular, biochemical and ecological cues. *BBA-Gen Subj.* **1862**, 2343–2353. https://doi.org/10.1016/j.bbagen.2018.03.028 (2018).
27. Wang, J. M. et al. Transcriptome-wide comparison of selenium hyperaccumulator and nonaccumulator Stanleya species provides new insight into key processes mediating the hyperaccumulation syndrome. *Plant. Biotechnol. J.* **16**, 1582–1594. https://doi.org/10.1111/pbi.12897 (2018).
28. Hawrylak-Nowak, B. Biological Activity of Selenium in Plants: Physiological and Biochemical Mechanisms of Phytotoxicity and Tolerance. In: (eds Hossain, M. A., Ahammed, G. J., Kolbert, Z., El-Ramady, H., Islam, T. & Schiavon, M.) Selenium and Nano-Selenium in Environmental Stress Management and Crop Quality Improvement. Sustainable Plant Nutrition in a Changing World. Springer, Cham. https://doi.org/10.1007/978-3-031-07063-1_17 (2022).
29. Heras, I. L., Palomo, M. & Madrid, Y. Selenoproteins: the key factor in selenium essentiality. State of the art analytical techniques for selenoprotein studies. *Anal. Bioanal Chem.* **400**, 1717–1727. https://doi.org/10.1007/s00216-011-4916-4 (2011).
30. Jalal, A. et al. Interaction of Mineral Nutrients and Plant Growth-Promoting Microbes for Biofortification of Different Cropping Systems. J Plant Growth Regul (2024). https://doi.org/10.1007/s00344-024-11380-1
31. Khan, Z. et al. The role of selenium and nano selenium on physiological responses in plant: a review. *Plant. Growth Regul.* **100**, 409–433. https://doi.org/10.1007/s10725-023-00988-0 (2023).
32. Erdal, S. & Turk, H. Cysteine-induced upregulation of nitrogen metabolism-related genes and enzyme activities enhance tolerance of maize seedlings to cadmium stress. *Environ. Exp. Bot.* **132**, 92–99. https://doi.org/10.1016/j.envexpbot.2016.08.014 (2016).
33. Fan, Z. J. et al. Effects of Nitrogen Application Amount on Soil Selenium Speciations, Physiological Characteristics and Yield of Triticales in Selenium-Enriched Area. *Russ J. Plant. Physiol.* **70**, 207. https://doi.org/10.1134/S1021443723602033 (2023).
34. Hu, C. et al. Selenium uptake, translocation, subcellular distribution and speciation in winter wheat in response to phosphorus application combined with three types of selenium fertilizer. *BMC Plant. Biol.* **23**, 224. https://doi.org/10.1186/s12870-023-04227-6 (2023).

35. Li, J. et al. Genome-wide analysis of the phosphate transporter gene family in oats: insights into phosphorus and water deficiency responses. *J. Appl. Genet.* https://doi.org/10.1007/s13353-025-00965-5 (2025).
36. Sun, Y. et al. Phosphate Transporter OsPT4, Ubiquitinated by E3 Ligase OsAIRP2, Plays a Crucial Role in Phosphorus and Nitrogen Translocation and Consumption in Germinating Seed. *Rice* **16**, 54. https://doi.org/10.1186/s12284-023-00666-9 (2023).
37. Elkelish, A. A. et al. Selenium protects wheat seedlings against salt stress-mediated oxidative damage by up-regulating antioxidants and osmolytes metabolism. *Plant. Physiol. Bioch.* **137**, 144–153. https://doi.org/10.1016/j.plaphy.2019.02.004 (2019).
38. Hao, X. et al. Hydrogen sulfide improves plant drought tolerance by regulating the homeostasis of reactive oxygen species. *Plant. Growth Regul.* **104**, 803–821. https://doi.org/10.1007/s10725-024-01197-z (2024).
39. Kaur, S., Sharma, S. & Singla, P. Selenium treatment alters the accumulation of osmolytes in arsenic-stressed rice (*Oryza sativa* L). *Environ. Sci. Pollut Res.* **31**, 10545–10564. https://doi.org/10.1007/s11356-024-31890-5 (2024).
40. Ulhassan, Z. et al. Selenium mitigates the chromium toxicity in *Brassicca napus* L. by ameliorating nutrients uptake, amino acids metabolism and antioxidant defense system. *Plant. Physiol. Bioch.* **145**, 142–152. https://doi.org/10.1016/j.plaphy.2019.10.035 (2019).
41. Hussein, H. A., Darwesh, O. M. & Mekki, B. B. Environmentally friendly nano-selenium to improve antioxidant system and growth of groundnut cultivars under sandy soil conditions. *Biocatal. Agric. Biotechnol.* **18**, 101080. https://doi.org/10.1016/j.bcab.2019.101080 (2018).
42. Zarbakhsh, S. & Shahsavar, A. R. Exogenous γ-aminobutyric acid improves the photosynthesis efficiency, soluble sugar contents, and mineral nutrients in pomegranate plants exposed to drought, salinity, and drought-salinity stresses. *BMC Plant. Biol.* **23**, 543. https://doi.org/10.1186/s12870-023-04568-2 (2023).
43. Angon, P. B. et al. Plant development and heat stress: role of exogenous nutrients and phytohormones in thermotolerance. *Discov Plants*. **1**, 17. https://doi.org/10.1007/s44372-024-00020-3 (2024).
44. Shahzad, R. et al. Iron oxide nanoparticles enhance alkaline stress resilience in bell pepper by modulating photosynthetic capacity, membrane integrity, carbohydrate metabolism, and cellular antioxidant defense. *BMC Plant. Biol.* **25**, 170. https://doi.org/10.1186/s12870-025-06180-y (2025).
45. Liang, C. J. & Zhang, B. J. Effect of exogenous calcium on growth, nutrients uptake and plasma membrane H^+-ATPase and Ca^{2+}-ATPase activities in soybean (*Glycine max*) seedlings under simulated acid rain stress. *Ecotox Environ. Safe.* **165**, 261–269. https://doi.org/10.1016/j.ecoenv.2018.09.019 (2018).
46. Zhou, T. et al. Spermidine improves antioxidant activity and energy metabolism in mung bean sprouts. *Food Chem.* **309**, 125759. https://doi.org/10.1016/j.foodchem.2019.125759 (2020).

Acknowledgements

This work was supported by Shandong postdoctoral innovation project (SDCX-ZG-202400134) and General Program of Education Department of Liaoning (LJKMZ20221465). Moreover, thanks to Novogene Technology Co, Ltd. (Beijing, China) for their supporting of GC-MS assisted derivatization test platform and in-house database of compounds.

Author contributions

Mei Lv and Junwei Wang conceived and designed the experiments. Mei Lv performed the experiments. Junwei Wang wrote the paper. Siyao Wang contributed to this work by drafting, editing, and revising the manuscript, overseeing project management and acquiring financial support. All authors read and approved the final manuscript.

Declarations

Competing interests

The authors declare no competing interests.

Additional information

Correspondence and requests for materials should be addressed to J.W., M.L. or S.W.

Reprints and permissions information is available at www.nature.com/reprints.

Publisher's note Springer Nature remains neutral with regard to jurisdictional claims in published maps and institutional affiliations.

Open Access This article is licensed under a Creative Commons Attribution-NonCommercial-NoDerivatives 4.0 International License, which permits any non-commercial use, sharing, distribution and reproduction in any medium or format, as long as you give appropriate credit to the original author(s) and the source, provide a link to the Creative Commons licence, and indicate if you modified the licensed material. You do not have permission under this licence to share adapted material derived from this article or parts of it. The images or other third party material in this article are included in the article's Creative Commons licence, unless indicated otherwise in a credit line to the material. If material is not included in the article's Creative Commons licence and your intended use is not permitted by statutory regulation or exceeds the permitted use, you will need to obtain permission directly from the copyright holder. To view a copy of this licence, visit http://creativecommons.org/licenses/by-nc-nd/4.0/.

© The Author(s) 2026